Leading Edge
Review

Cell

A Tale of Chromatin and Transcription in 100 Structures

Patrick Cramer[1,*]
[1]Department of Molecular Biology, Max Planck Institute for Biophysical Chemistry, Am Fassberg 11, 37077 Göttingen, Germany
*Correspondence: patrick.cramer@mpibpc.mpg.de
http://dx.doi.org/10.1016/j.cell.2014.10.047

To celebrate a century of X-ray crystallography, I describe how 100 crystal structures influenced chromatin and transcription research.

Introduction

When Max von Laue first illuminated a crystal with X-rays 100 years ago, it was unclear what the obtained diffraction pattern meant. William Henry Bragg and his son Lawrence, however, soon realized that X-ray diffraction provided information about the inner structure of crystals. After decades of elaboration, X-ray crystallography advanced to become the most widely used method for the determination of 3D structures. Its application to biological macromolecules fostered the development of molecular biology in the second half of the 20th century. Crystallography defined biological paradigms such as molecular recognition, enzymatic catalysis, and allosteric regulation.

Until about 30 years ago, researchers could still follow publication of all new crystal structures of biomolecules. But then the pace at which new structures were solved increased rapidly due to the advent of new enabling techniques. Proteins were obtained in recombinant form, and nucleic acids were synthesized in large quantities. Crystals were cryo-cooled to slow down radiation damage. Synchrotron X-ray sources improved, and fast X-ray detection devices emerged. Modern computers and better software for structure determination became available. By now, 100,000 structures have been deposited in the protein database. Many of these revealed the inner workings of molecular machines, allowing researchers to rationalize phenotypes of mutations and to engineer biological processes.

Crystal structures can be like landmarks. They can guide us on our way toward a better understanding of a biological process (Shi, 2014 [this issue of *Cell*]). Landmark structures not only disclose some of life's secrets, but they also open up new frontiers. Here, I describe many of the structures that I consider to be landmark structures in the biology of chromatin, transcription, and epigenetics. I hope the resulting list of about 100 crystallographic structures, along with several structures obtained by other methods, exemplifies how structural information influenced the community and led to new concepts.

How DNA Is Structured

The proposal of the double-helical structure of DNA relied on X-ray diffraction patterns of DNA fibers obtained in the middle of the last century (Watson and Crick, 1953) (Figure 1). The direct observation of a nucleic acid duplex, however, had to await the crystal structure of a transfer RNA (tRNA) from yeast in 1974 (Robertus et al., 1974) (Figure 1). The structure of a B-DNA duplex was solved only after DNA synthesis methods became available (Wing et al., 1980) (Figure 1). Crystal structures of DNA in A-form (Shakked et al., 1981) and Z-form (Wang et al., 1979) highlighted the sequence-dependent conformational flexibility of DNA.

In eukaryotic nuclei, DNA is packaged with histone proteins into chromatin. The fundamental unit of chromatin, the nucleosome core particle, was elucidated structurally in 1984 at a resolution of 7 Å (Richmond et al., 1984). When the resolution reached 2.8 Å, a detailed view of the nucleosome emerged that revealed the DNA conformation and DNA interactions with histones (Luger et al., 1997). The nucleosome core structure confirmed the structure of the free histone octamer (Arents et al., 1991). It further showed that the histone protein tails emerged between and around DNA duplexes to become available for interactions with other nucleosomes or chromatin.

The structure of higher-order chromatin is dynamic, but a complex of four nucleosomes could be crystallized and showed two stacks of nucleosomes and DNA that zigzagged between them (Schalch et al., 2005). Electron microscopy revealed how such tetranucleosome units may be arranged within a 30 nm fiber of chromatin (Song et al., 2014) and provided evidence for helical order in such fibers (Scheffer et al., 2011). Another electron microscopic study provided an alternative fiber model (Robinson et al., 2006). These results explained how extended DNA molecules can be packaged in the cell nucleus but also provided models for how chromatin regulates the accessibility of genes and their transcription. Whereas a compact chromatin structure can cause gene repression, gene activation requires chromatin opening and assembly of the transcription machinery at the promoter.

How DNA Is Recognized

To enable transcription, cells use transcription factors that bind to specific DNA sites. The first crystal structures of transcription factors included the bacterial catabolite activator protein CAP (McKay and Steitz, 1981) (Figure 1) and the bacteriophage lambda proteins cro (Anderson et al., 1981) and repressor (Pabo and Lewis, 1982). These structures contained helix-turn-helix regions that were involved in DNA binding and led to the concept of DNA-binding protein motifs. The studies of the bacteriophage proteins required protein overexpression because these transcription factors could not be isolated from natural sources in quantities required for structural studies.

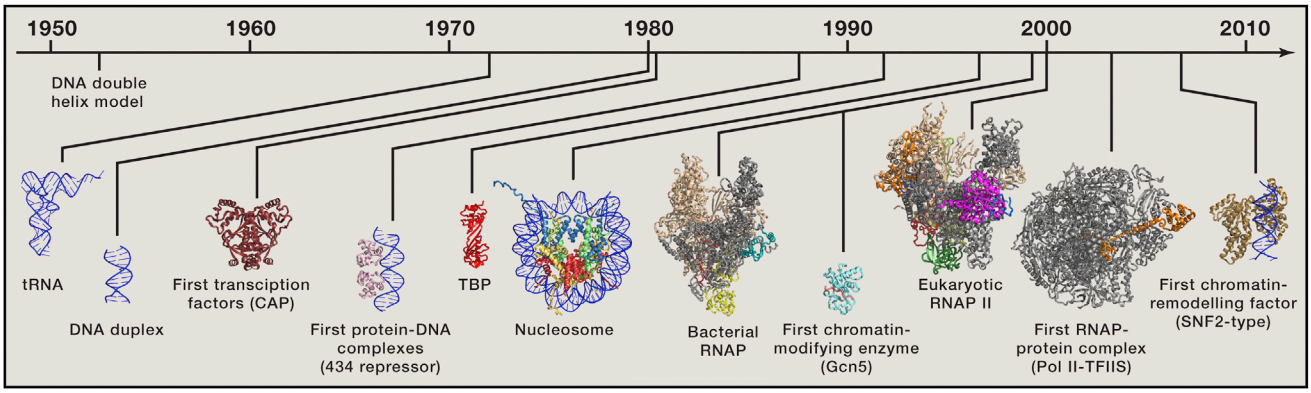

Figure 1. A Selection of Landmark Crystal Structures in the Biology of Chromatin and Transcription

From left to right, the depicted structures are yeast tRNA, a DNA duplex, the bacterial transcription factor CAP, the bacteriophage 434 repressor protein in complex with DNA, the eukaryotic TATA-binding protein TBP, the nucleosome, the bacterial RNA polymerase, the histone acetyltransferase Gcn5, the eukaryotic RNA polymerase 10-subunit core enzyme, the complete 12-subunit RNA polymerase II complex in complex with transcription factor TFIIS, and an archaeal Swi/Snf-type ATPase resembling the catalytic subunit found in many chromatin remodeling complexes. DNA is shown in blue, and proteins are depicted as ribbon models in different colors. For details, please refer to the text.

Structures of DNA-bound transcription factors led to the concept of sequence-specific DNA recognition. DNA complexes of the repressor proteins from bacteriophages 434 (Anderson et al., 1987) (Figure 1) and lambda (Jordan and Pabo, 1988) and of the 434 cro protein (Wolberger et al., 1988) revealed protein helices bound in the DNA major groove. DNA-binding helices were also observed in structures of homeodomains (Kissinger et al., 1990; Otting et al., 1990; Qian et al., 1989). In a ''leucine zipper'' of the GCN4 factor, protein helices in the DNA major groove were extended and used for factor dimerization (Ellenberger et al., 1992; König and Richmond, 1993). The transcription factors recognized target sequences via interactions of amino acid residues with DNA base edges. Such ''direct readout'' can be complemented by ''indirect readout'' of the DNA conformation via protein-DNA backbone contacts (Lesser et al., 1990; Otwinowski et al., 1988).

Later protein-DNA complex structures revealed a variety of DNA-binding structural motifs. The transcription factor NF-κB uses a β barrel fold to contact DNA via protein loops (Becker et al., 1998; Ghosh et al., 1995; Müller et al., 1995). Transcription factors of the zinc finger family recognize DNA with small protein folds that are stabilized by zinc ions (Fairall et al., 1993; Luisi et al., 1991; Marmorstein et al., 1992; Pavletich and Pabo, 1991). Zinc fingers were later used for the design of proteins with new DNA-binding specificities (Choo et al., 1994). This catalyzed the development of protein and genome engineering as new research fields. Zinc fingers were also present in Klf4 (Schuetz et al., 2011), which, together with transcription factors Oct4, Sox2, and c-Myc, enables reprogramming of the genome and generation of induced pluripotent stem cells.

Crystallography also showed how transcription factors bind to adjacent DNA sites for combinatorial gene regulation. The DNA-bound structures of yeast MATα2 interacting with MATa1 (Li et al., 1995) and with MCM1 (Tan and Richmond, 1998) revealed factor-factor interactions that underlie synergistic DNA binding. This concept held for human transcription factors (Piper et al., 1999). Oct4 and Sox2 can also bind to neighboring DNA sites (Reményi et al., 2003). Crystallography also led to a model of an ''enhanceosome'' containing eight transcription factors bound to DNA (Panne et al., 2007). Here, binding of one factor induces a DNA conformation that promotes binding of a neighboring factor.

Transcription factors can also bend DNA dramatically. The bacterial CAP protein bends DNA by 90 degrees to enable specific DNA recognition (Schultz et al., 1991). The eukaryotic TATA box-binding protein (TBP) also introduces a 90 degree bend into DNA (Kim et al., 1993a, 1993b). The integration host factor (Rice et al., 1996) and the mitochondrial transcription factor A (Ngo et al., 2011; Rubio-Cosials et al., 2011) can even bend DNA by 180 degrees, inducing a U-turn. To achieve DNA bending, proteins can use two strategies. They can insert amino acid residues like wedges between DNA base pairs to disrupt base stacking and may also neutralize backbone charges on one side of DNA, which induces bending due to the repulsion of phosphates on the opposite strand.

How DNA Binding Is Regulated

Crystallography further established concepts that explained bacterial gene regulation. In the *trp* operon, the Trp repressor protein inhibits expression of enzymes required for tryptophan biosynthesis when enough of the amino acid is available. The structure of the Trp repressor revealed a homodimer with a DNA-binding helix in each monomer (Schevitz et al., 1985). Binding of the regulator tryptophan alters the relative position of the two helices to enable DNA binding and gene repression (Otwinowski et al., 1988). These studies also showed that water molecules in the protein-DNA interface may contribute to sequence-specific DNA recognition.

Many transcription factors contain not only a DNA-binding domain but also additional domains that can activate transcription or bind other transcription factors or small-molecule regulators. In the bacterial *lac* operon, the Lac repressor protein binds DNA to control the expression of enzymes involved in lactose metabolism. The lac repressor contains a domain that binds

the regulator lactose (Friedman et al., 1995) and a domain that binds DNA (Bell and Lewis, 2000; Lewis et al., 1996). The regulator allosterically changes the orientation of the DNA-binding domains, leading to DNA dissociation and gene activation.

Eukaryotic transcription factors are generally also modular. The nuclear receptor for the hormone estrogen comprises a DNA-binding domain (Schwabe et al., 1993) and a hormone-binding domain (Brzozowski et al., 1997). Binding of estrogen influences receptor dimerization and its interaction with other factors that regulate transcription. The tumor suppressor p53 contains a tetramerization domain that clamps four p53 subunits together (Clore et al., 1994) and a DNA-binding domain that harbors tumorigenic mutations that can impair DNA binding (Cho et al., 1994).

Transcription factors are often regulated by nuclear localization. For example, the inhibitory protein I-κB retains the transcription factor NF-κB in the cytoplasm by masking its nuclear localization sequence (Huxford et al., 1998). External signals remove I-κB, leading to nuclear import of NF-κB, DNA binding, and gene activation. Similarly, external signals trigger phosphorylation of cytosolic STAT transcription factors (Becker et al., 1998), which leads to factor dimerization, nuclear import, DNA binding, and gene activation.

How DNA Directs RNA Synthesis: Single-Subunit RNA Polymerases

It took until the late 1990s to obtain a crystallographic view of transcription. The shape of the single-subunit DNA-dependent RNA polymerase from bacteriophage T7 was observed in a medium-resolution crystallographic study (Sousa et al., 1993). The crystal structure of T7 RNA polymerase revealed an active center cleft and a domain that binds promoter DNA and enables sequence-specific initiation of RNA synthesis (Jeruzalmi and Steitz, 1998; Cheetham et al., 1999). In the structure of a T7 RNA polymerase transcribing complex, the DNA template strand formed a hybrid duplex with a transcript of three nucleotides at the active site (Cheetham and Steitz, 1999). This suggested that the polymerase could only hold a three base pair DNA-RNA hybrid, but later structures of the T7 elongation complex revealed extensive refolding of the polymerase, which then accommodated a seven to eight base pair hybrid (Tahirov et al., 2002; Yin and Steitz, 2002).

These studies established many concepts in DNA-directed RNA synthesis. They highlighted the importance of promoter recognition and showed how ribonucleotide substrates are selected over deoxyribonucleotides to prevent synthesis of DNA. Addition of nucleotides to the RNA occurs in two steps by first binding the substrate nucleoside triphosphate to a preinsertion site and then moving it to the insertion site for catalysis (Temiakov et al., 2004). Details of RNA synthesis were revealed by X-ray studies of the single-subunit RNA polymerase from bacteriophage N4 (Basu and Murakami, 2013).

Eukaryotic cells also contain a single-subunit RNA polymerase, the polymerase transcribing the mitochondrial genome. Mitochondrial RNA polymerase structurally resembles T7 RNA polymerase but contains an additional region for promoter binding (Ringel et al., 2011). In contrast to T7 RNA polymerase, mitochondrial RNA polymerase, however, does not refold during the transition from transcription initiation to elongation (Schwinghammer et al., 2013).

How DNA Is Transcribed in Cells: Multisubunit RNA Polymerases

The first structures of cellular RNA polymerases were obtained at the turn of the millennium. The structure of bacterial RNA polymerase from *Thermus aquaticus* (Zhang et al., 1999) was followed by the structure of yeast RNA polymerase II (Pol II), which synthesizes messenger RNA (Cramer et al., 2000, 2001) (Figure 1). The structures revealed functional elements and enabled structure-function analysis of cellular transcription. They also suggested that catalysis followed a two-metal ion mechanism (Cramer et al., 2000), as proposed for all nucleotide polymerases (Steitz and Steitz, 1993). Comparison of bacterial and eukaryotic RNA polymerases revealed a conserved multisubunit architecture and an active center cleft with a flexible bridge helix for the translocation of the polymerase relative to DNA.

The structure of a Pol II transcription elongation complex showed that the polymerase clamp domain closed over a DNA-RNA hybrid of eight to nine base pairs during transcription elongation and suggested the basis for nucleic acid strand separation during transcription (Gnatt et al., 2001). Later structures of bacterial RNA polymerase and Pol II transcription elongation complexes with bound nucleoside triphosphate substrate (Vassylyev et al., 2007; Wang et al., 2006) revealed that folding of the polymerase trigger loop closed the active site and suggested mechanisms of substrate selection. The same mechanisms likely occur in archaeal RNA polymerases, which show a remarkable similarity to Pol II (Hirata et al., 2008; Korkhin et al., 2009).

The first structure of Pol II with a bound transcription factor, the elongation factor TFIIS, showed that a single "tunable" active site was used both for RNA synthesis and RNA cleavage and indicated the mechanism of proofreading during transcription (Kettenberger et al., 2003) (Figure 1). Electron microscopy of an analogous bacterial complex revealed a similar topology (Opalka et al., 2003). The structure of an "arrested" Pol II elongation complex with a backtracked RNA provided insights into how TFIIS rescues polymerase that stalled during transcription (Cheung and Cramer, 2011). Crystal structures of a second eukaryotic RNA polymerase, Pol I, showed that a subunit corresponding to TFIIS was located at the active center of this enzyme (Engel et al., 2013; Fernández-Tornero et al., 2013).

Transcription is coordinated with cotranscriptional events such as RNA processing. This coordination is to a large extent achieved by binding of factors to the flexible C-terminal domain (CTD) of Pol II. Changes in CTD phosphorylation lead to an exchange of protein factors during transcription. The first structures of CTD peptides bound to CTD-binding proteins showed that the CTD adopts multiple conformations and revealed the basis for phosphorylation-specific binding (Fabrega et al., 2003; Meinhart and Cramer, 2004; Verdecia et al., 2000). Crystallography also revealed the mechanisms and the determinants for substrate specificity of CTD kinases (Baumli et al., 2012; Baumli et al., 2008; Bösken et al., 2014; Lolli et al., 2004; Schneider et al., 2011; Tahirov et al., 2010) and CTD phosphatases (Ghosh et al., 2008; Kamenski et al., 2004; Xiang et al., 2010).

How Transcription Starts

For the initiation of transcription, RNA polymerases cooperate with initiation factors to locate and open promoter DNA. The structure of the Pol II initiation factor TBP revealed a saddle-shaped molecule (Nikolov et al., 1992) (Figure 1) that bound the DNA minor groove and bent DNA by 90 degrees (Kim et al., 1993a, 1993b). The resulting TBP-DNA complex can recruit initiation factors TFIIA (Geiger et al., 1996; Tan et al., 1996) and TFIIB (Nikolov et al., 1995) on either side. Electron microscopy revealed the overall architectures of the large multiprotein initiation factors TFIID (Andel et al., 1999; Bieniossek et al., 2013; Cianfrocco et al., 2013; Leurent et al., 2002) and TFIIH (Chang and Kornberg, 2000; Gibbons et al., 2012; Schultz et al., 2000). Crystal structures for individual parts of TFIID, TFIIE, TFIIF, and TFIIH were reported, including an archaeal homolog of the ATPase in TFIIH (Fan et al., 2006) that functions in DNA opening.

An understanding of transcription initiation, however, had to await structures of initiation factor complexes with RNA polymerases. An initial structure of a partial Pol II-TFIIB complex (Bushnell et al., 2004) was consistent with crosslinking results (Chen and Hahn, 2003) and revealed a domain of TFIIB that bound Pol II to recruit it to the promoter. The structure of the Pol II-TFIIB complex (Kostrewa et al., 2009; Liu et al., 2010) enabled modeling of initiation complexes with closed double-stranded and open DNA. A subsequent structure of a Pol II-TFIIB complex with bound DNA and an initial RNA transcript showed that TFIIB alters the polymerase active site to allosterically activate RNA synthesis (Sainsbury et al., 2013).

Bacterial transcription initiation relies on sigma factors. The structure of a free sigma factor revealed its modular nature (Malhotra et al., 1996). Structures of RNA polymerase with bound sigma factor (Murakami et al., 2002b; Vassylyev et al., 2002) and with sigma factor and promoter DNA (Murakami et al., 2002a) showed that sigma factor bridges between polymerase and the promoter and suggested how sigma factor domains recognize DNA sequence elements. When promoter DNA is unwound, one sigma factor domain traps the nontemplate single strand of DNA (Feklistov and Darst, 2011). An alternative sigma factor is able to stabilize a flipped-out base from the nontemplate strand during DNA melting (Campagne et al., 2014). Structures of bacterial transcription initiation complexes showed how RNA polymerase and sigma factor cooperate to recognize promoter sequences, unwind DNA, and "preorganize" the template strand for RNA chain initiation (Zhang et al., 2012).

The initiation factors sigma and TFIIB perform similar functions, including DNA binding and opening and defining the start site of transcription. Comparison of bacterial and eukaryotic structures showed that sigma factor and TFIIB interact with roughly the same parts of their RNA polymerases but have unrelated folds, arguing for convergent evolution. Recently, electron microscopy and crosslinking provided the location of additional initiation factors in human and yeast Pol II initiation complexes (Grünberg et al., 2012; He et al., 2013; Mühlbacher et al., 2014; Murakami et al., 2013), enabling further crystallographic studies of transcription initiation.

How Transcription Initiation Is Regulated

Bacterial transcription can be regulated by direct interactions of transcription factors with the general transcription machinery and DNA. The CAP factor activates transcription by binding DNA and an adjacent domain of the polymerase, thereby recruiting the polymerase to the promoter (Benoff et al., 2002). Similarly, a protein of bacteriophage lambda activates transcription by binding to DNA and an adjacent domain of sigma (Jain et al., 2004). Eukaryotic transcription factors normally bind to coactivator complexes, which then bind the general transcription machinery. Coactivator binding requires activation domains, which are often unstructured in their free state but can adopt short helical structures upon coactivator binding (Brzovic et al., 2011; Kussie et al., 1996; Radhakrishnan et al., 1997). Vice versa, a coactivator can also form a α helix to bind a transcription factor (Shiau et al., 1998).

Many transcription factors bind to the coactivator complex Mediator, which consists of 25–35 subunits arranged in four modules. The crystal structure of the Mediator head module revealed an intricate fold with surfaces for interactions with Pol II and other Mediator modules (Imasaki et al., 2011; Larivière et al., 2012; Robinson et al., 2012). Recent electron microscopy revealed the central location of the head module within the overall Mediator architecture (Tsai et al., 2014; Wang et al., 2014). The mechanisms by which Mediator influences transcription remain to be explored, but there is evidence for a conformational change in Mediator induced by binding of a transcription activator (Meyer et al., 2010; Taatjes et al., 2002).

Transcription initiation is also regulated by methylation of DNA upstream of the promoter. In higher cells, this often occurs in CpG islands, which are DNA regions enriched for CpG dinucleotides. Hypermethylation of CpG islands generally leads to transcription repression. In a structure of a methyltransferase-DNA substrate complex, the target base was flipped out of the DNA double helix and inserted into the enzyme's active site (Klimasauskas et al., 1994). A human DNA methyltransferase uses additional domains to ensure that only hemimethylated CpG dinucleotides undergo methylation after replication, as seen in the enzyme-DNA complex structure (Song et al., 2011; Song et al., 2012).

How Chromatin Regulates Transcription

To make chromatin accessible for transcription, remodeling complexes use ATP hydrolysis to change nucleosome position and structure. Many remodelers contain a Swi/Snf family ATPase that induces DNA translocation with respect to histones (Dürr et al., 2005; Thomä et al., 2005) (Figure 1). A combination of structural techniques provided the architecture of chromatin remodelers ISW1a (Yamada et al., 2011), INO80 (Saravanan et al., 2012; Tosi et al., 2013), and SWR1 (Nguyen et al., 2013) and indicated how these machines bind nucleosomes, although the structure of the "remodeled nucleosome state" has remained elusive. Remodeling complexes not only bind nucleosomes—they can also be regulated by nucleosomes allosterically (Clapier and Cairns, 2012; Hauk et al., 2010; Racki et al., 2014).

Proper nucleosome assembly by histone chaperones is required to repress cryptic transcription that can produce aberrant RNAs from nonpromoter regions. X-ray studies unraveled

chaperone structures and showed that chaperones disrupt histone interfaces or mimic nucleosomal DNA to prevent promiscuous histone interactions prior to their assembly into nucleosomes (Elsässer et al., 2012; English et al., 2006; Hondele et al., 2013; Hu et al., 2011; Park and Luger, 2006). Certain assembly factors incorporate histone variants into nucleosomes at specific sites. The histone variant H2A.Z changes nucleosome structure at active promoters (Suto et al., 2000) and is removed by a specific chaperone (Obri et al., 2014), and nucleosomes containing the centromeric histone H3 variant are apparently destabilized compared to canonical nucleosomes (Tachiwana et al., 2011).

Structural studies also revealed details on how proteins recognize nucleosomes. A structure of a nucleosome in complex with RCC1, a regulator of chromatin condensation, showed how this protein recognizes both histones and DNA to specifically bind nucleosomes (Makde et al., 2010). Another nucleosome structure in complex with the gene-silencing factor Sir3 indicated how protein-nucleosome interactions are regulated by modifications in histone tails (Armache et al., 2011).

How Chromatin Marks Function

Covalent histone modifications provide another layer of gene regulation (Strahl and Allis, 2000). Histone modifications include acetylation, methylation, phosphorylation, and ubiquitination and can be associated with active transcription or repression. Enzymes that set or remove these marks are known as "writers" and "erasers," respectively. The structure of the histone acetyltransferase Gcn5 provided insights into how chromatin marks are written (Rojas et al., 1999) (Figure 1). The structure of a portion of the acetyltransferase p300 explained mutations associated with human cancers (Liu et al., 2008). The subunit organization of the large acetyltransferase complex NuA4 and its mode of interaction with the nucleosome were revealed by electron microscopy (Chittuluru et al., 2011). Crystal structures of histone methyltransferases revealed their mechanism and how specificity for histones was achieved (Kwon et al., 2003; Min et al., 2002; Wilson et al., 2002; Xiao et al., 2003; Zhang et al., 2002).

Crystallography also showed how eraser enzymes work. The structure of a bacterial homolog of a histone deacetylase (Finnin et al., 1999) was followed by structures of the NAD-dependent Sir2 enzyme (Avalos et al., 2002; Finnin et al., 2001; Min et al., 2001) and eukaryotic zinc-dependent histone deacetylases (Somoza et al., 2004; Vannini et al., 2004). Histone demethylase structures of the LSD1 (Chen et al., 2006; Stavropoulos et al., 2006; Yang et al., 2006) and JmJ (Ng et al., 2007) classes revealed the basis for substrate specificity. The structure of the four-subunit deubiquitination module of the SAGA complex provided the basis for substrate specificity and activation of this eraser (Köhler et al., 2010; Samara et al., 2010).

Histone marks can recruit proteins via specific "reader" domains. The bromodomain binds acetylated lysine residues, as observed for the factors P/CAF, Taf1, and Gcn5 (Dhalluin et al., 1999; Jacobson et al., 2000; Owen et al., 2000). The chromodomain binds methylated lysines, as exemplified by the HP1 chromodomain bound to a histone H3 peptide methylated at lysine-9 (Jacobs and Khorasanizadeh, 2002). The PHD finger domain also binds a methylated lysine residue by trapping it into an aromatic cage that is lined with residues mutated in cancer (Li et al., 2006; Peña et al., 2006). The pockets in reader and eraser proteins were consequently explored for drug design (Filippakopoulos et al., 2010). Multiple histone marks can be read by a single reader domain (Morinière et al., 2009) or by combinatorial binding of readers (Jacobson et al., 2000; Tsai et al., 2010; Xi et al., 2011). Multiple histone marks influence transcription activity, for example, via the initiation factor TFIID that binds histone tails with marks for active transcription (Vermeulen et al., 2007).

Toward Structural Cell Biology

In the coming years, X-ray crystallography will likely continue to provide landmark structures that elucidate unknown mechanisms in chromatin and transcription biology. However, many proteins that function in chromatin and transcription are modular by design. To resolve the structure of flexible factors and transient multicomponent complexes, crystallography will often be integrated with complementary techniques. Of particular importance will be electron microscopy, which enables placement of crystal structures of complex components but can now also reach high resolution that enables building of atomic models (Kühlbrandt, 2014; Wong et al., 2014). Crosslinking and mass spectrometry (Gingras et al., 2007; Serpa et al., 2012) will be routinely used to derive the relative position of known structures and to support models obtained by a combination of electron microscopy and crystallography.

A central future challenge will be the analysis of molecular structures within their cellular context and of structural changes in space and time. Advanced light microscopy techniques can now resolve detailed structures of assemblies such as nuclear pore complexes (Szymborska et al., 2013) or the cytoskeleton (Xu et al., 2013). A combination of in vivo crosslinking with deep sequencing and computer simulations can elucidate the overall folding of chromosomes (Naumova et al., 2013). Electron tomography provides three-dimensional images of the nuclear pore complex (Beck et al., 2004; Bui et al., 2013) or polysomes (Brandt et al., 2009).

We are witnessing the advent of a new research field that may be referred to as structural cell biology. Structural biologists may soon tackle most fundamental questions in biology. What is the conformational space for genomes, and how is it explored and utilized during gene activation and cell differentiation? What is the three-dimensional structure of genes and how does it change during transcription? What is the dynamic architecture of transient RNA assemblies with multiple proteins? Answers to these questions will require the development of new techniques and algorithms to bridge resolution gaps, to integrate structural data from multiple sources, and to embed structures into their biological context.

ACKNOWLEDGMENTS

I thank members of our laboratory and the following colleagues who provided comments: David Allis, Karim-Jean Armache, Alan Cheung, Richard Ebright, Andreas Ladurner, Robert Landick, Karolin Luger, Ronen Marmorstein, Christoph Müller, Dinshaw Patel, Alessandro Vannini, and Cynthia Wolberger. I thank Lucas Farnung for help with preparing the figure.

REFERENCES

Andel, F., 3rd, Ladurner, A.G., Inouye, C., Tjian, R., and Nogales, E. (1999). Three-dimensional structure of the human TFIID-IIA-IIB complex. Science *286*, 2153–2156.

Anderson, W.F., Ohlendorf, D.H., Takeda, Y., and Matthews, B.W. (1981). Structure of the cro repressor from bacteriophage lambda and its interaction with DNA. Nature *290*, 754–758.

Anderson, J.E., Ptashne, M., and Harrison, S.C. (1987). Structure of the repressor-operator complex of bacteriophage 434. Nature *326*, 846–852.

Arents, G., Burlingame, R.W., Wang, B.C., Love, W.E., and Moudrianakis, E.N. (1991). The nucleosomal core histone octamer at 3.1 A resolution: a tripartite protein assembly and a left-handed superhelix. Proc. Natl. Acad. Sci. USA *88*, 10148–10152.

Armache, K.J., Garlick, J.D., Canzio, D., Narlikar, G.J., and Kingston, R.E. (2011). Structural basis of silencing: Sir3 BAH domain in complex with a nucleosome at 3.0 Å resolution. Science *334*, 977–982.

Avalos, J.L., Celic, I., Muhammad, S., Cosgrove, M.S., Boeke, J.D., and Wolberger, C. (2002). Structure of a Sir2 enzyme bound to an acetylated p53 peptide. Mol. Cell *10*, 523–535.

Basu, R.S., and Murakami, K.S. (2013). Watching the bacteriophage N4 RNA polymerase transcription by time-dependent soak-trigger-freeze X-ray crystallography. J. Biol. Chem. *288*, 3305–3311.

Baumli, S., Lolli, G., Lowe, E.D., Troiani, S., Rusconi, L., Bullock, A.N., Debreczeni, J.E., Knapp, S., and Johnson, L.N. (2008). The structure of P-TEFb (CDK9/cyclin T1), its complex with flavopiridol and regulation by phosphorylation. EMBO J. *27*, 1907–1918.

Baumli, S., Hole, A.J., Wang, L.Z., Noble, M.E., and Endicott, J.A. (2012). The CDK9 tail determines the reaction pathway of positive transcription elongation factor b. Structure *20*, 1788–1795.

Beck, M., Förster, F., Ecke, M., Plitzko, J.M., Melchior, F., Gerisch, G., Baumeister, W., and Medalia, O. (2004). Nuclear pore complex structure and dynamics revealed by cryoelectron tomography. Science *306*, 1387–1390.

Becker, S., Groner, B., and Müller, C.W. (1998). Three-dimensional structure of the Stat3beta homodimer bound to DNA. Nature *394*, 145–151.

Bell, C.E., and Lewis, M. (2000). A closer view of the conformation of the Lac repressor bound to operator. Nat. Struct. Biol. *7*, 209–214.

Benoff, B., Yang, H., Lawson, C.L., Parkinson, G., Liu, J., Blatter, E., Ebright, Y.W., Berman, H.M., and Ebright, R.H. (2002). Structural basis of transcription activation: the CAP-alpha CTD-DNA complex. Science *297*, 1562–1566.

Bieniossek, C., Papai, G., Schaffitzel, C., Garzoni, F., Chaillet, M., Scheer, E., Papadopoulos, P., Tora, L., Schultz, P., and Berger, I. (2013). The architecture of human general transcription factor TFIID core complex. Nature *493*, 699–702.

Bösken, C.A., Farnung, L., Hintermair, C., Merzel Schachter, M., Vogel-Bachmayr, K., Blazek, D., Anand, K., Fisher, R.P., Eick, D., and Geyer, M. (2014). The structure and substrate specificity of human Cdk12/Cyclin K. Nat. Commun. *5*, 3505.

Brandt, F., Etchells, S.A., Ortiz, J.O., Elcock, A.H., Hartl, F.U., and Baumeister, W. (2009). The native 3D organization of bacterial polysomes. Cell *136*, 261–271.

Brzovic, P.S., Heikaus, C.C., Kisselev, L., Vernon, R., Herbig, E., Pacheco, D., Warfield, L., Littlefield, P., Baker, D., Klevit, R.E., and Hahn, S. (2011). The acidic transcription activator Gcn4 binds the mediator subunit Gal11/Med15 using a simple protein interface forming a fuzzy complex. Mol. Cell *44*, 942–953.

Brzozowski, A.M., Pike, A.C., Dauter, Z., Hubbard, R.E., Bonn, T., Engström, O., Ohman, L., Greene, G.L., Gustafsson, J.A., and Carlquist, M. (1997). Molecular basis of agonism and antagonism in the oestrogen receptor. Nature *389*, 753–758.

Bui, K.H., von Appen, A., DiGuilio, A.L., Ori, A., Sparks, L., Mackmull, M.T., Bock, T., Hagen, W., Andrés-Pons, A., Glavy, J.S., and Beck, M. (2013). Integrated structural analysis of the human nuclear pore complex scaffold. Cell *155*, 1233–1243.

Bushnell, D.A., Westover, K.D., Davis, R.E., and Kornberg, R.D. (2004). Structural basis of transcription: an RNA polymerase II-TFIIB cocrystal at 4.5 Angstroms. Science *303*, 983–988.

Campagne, S., Marsh, M.E., Capitani, G., Vorholt, J.A., and Allain, F.H. (2014). Structural basis for -10 promoter element melting by environmentally induced sigma factors. Nat. Struct. Mol. Biol. *21*, 269–276.

Chang, W.H., and Kornberg, R.D. (2000). Electron crystal structure of the transcription factor and DNA repair complex, core TFIIH. Cell *102*, 609–613.

Cheetham, G.M., and Steitz, T.A. (1999). Structure of a transcribing T7 RNA polymerase initiation complex. Science *286*, 2305–2309.

Cheetham, G.M., Jeruzalmi, D., and Steitz, T.A. (1999). Structural basis for initiation of transcription from an RNA polymerase-promoter complex. Nature *399*, 80–83.

Chen, H.T., and Hahn, S. (2003). Binding of TFIIB to RNA polymerase II: Mapping the binding site for the TFIIB zinc ribbon domain within the preinitiation complex. Mol. Cell *12*, 437–447.

Chen, Y., Yang, Y., Wang, F., Wan, K., Yamane, K., Zhang, Y., and Lei, M. (2006). Crystal structure of human histone lysine-specific demethylase 1 (LSD1). Proc. Natl. Acad. Sci. USA *103*, 13956–13961.

Cheung, A.C., and Cramer, P. (2011). Structural basis of RNA polymerase II backtracking, arrest and reactivation. Nature *471*, 249–253.

Chittuluru, J.R., Chaban, Y., Monnet-Saksouk, J., Carrozza, M.J., Sapountzi, V., Selleck, W., Huang, J., Utley, R.T., Cramet, M., Allard, S., et al. (2011). Structure and nucleosome interaction of the yeast NuA4 and Piccolo-NuA4 histone acetyltransferase complexes. Nat. Struct. Mol. Biol. *18*, 1196–1203.

Cho, Y., Gorina, S., Jeffrey, P.D., and Pavletich, N.P. (1994). Crystal structure of a p53 tumor suppressor-DNA complex: understanding tumorigenic mutations. Science *265*, 346–355.

Choo, Y., Sánchez-García, I., and Klug, A. (1994). In vivo repression by a site-specific DNA-binding protein designed against an oncogenic sequence. Nature *372*, 642–645.

Cianfrocco, M.A., Kassavetis, G.A., Grob, P., Fang, J., Juven-Gershon, T., Kadonaga, J.T., and Nogales, E. (2013). Human TFIID binds to core promoter DNA in a reorganized structural state. Cell *152*, 120–131.

Clapier, C.R., and Cairns, B.R. (2012). Regulation of ISWI involves inhibitory modules antagonized by nucleosomal epitopes. Nature *492*, 280–284.

Clore, G.M., Omichinski, J.G., Sakaguchi, K., Zambrano, N., Sakamoto, H., Appella, E., and Gronenborn, A.M. (1994). High-resolution structure of the oligomerization domain of p53 by multidimensional NMR. Science *265*, 386–391.

Cramer, P., Bushnell, D.A., Fu, J., Gnatt, A.L., Maier-Davis, B., Thompson, N.E., Burgess, R.R., Edwards, A.M., David, P.R., and Kornberg, R.D. (2000). Architecture of RNA polymerase II and implications for the transcription mechanism. Science *288*, 640–649.

Cramer, P., Bushnell, D.A., and Kornberg, R.D. (2001). Structural basis of transcription: RNA polymerase II at 2.8 angstrom resolution. Science *292*, 1863–1876.

Dhalluin, C., Carlson, J.E., Zeng, L., He, C., Aggarwal, A.K., and Zhou, M.M. (1999). Structure and ligand of a histone acetyltransferase bromodomain. Nature *399*, 491–496.

Dürr, H., Körner, C., Müller, M., Hickmann, V., and Hopfner, K.P. (2005). X-ray structures of the Sulfolobus solfataricus SWI2/SNF2 ATPase core and its complex with DNA. Cell *121*, 363–373.

Ellenberger, T.E., Brandl, C.J., Struhl, K., and Harrison, S.C. (1992). The GCN4 basic region leucine zipper binds DNA as a dimer of uninterrupted alpha helices: crystal structure of the protein-DNA complex. Cell *71*, 1223–1237.

Elsässer, S.J., Huang, H., Lewis, P.W., Chin, J.W., Allis, C.D., and Patel, D.J. (2012). DAXX envelops a histone H3.3-H4 dimer for H3.3-specific recognition. Nature *491*, 560–565.

Engel, C., Sainsbury, S., Cheung, A.C., Kostrewa, D., and Cramer, P. (2013). RNA polymerase I structure and transcription regulation. Nature *502*, 650–655.

English, C.M., Adkins, M.W., Carson, J.J., Churchill, M.E., and Tyler, J.K. (2006). Structural basis for the histone chaperone activity of Asf1. Cell *127*, 495–508.

Fabrega, C., Shen, V., Shuman, S., and Lima, C.D. (2003). Structure of an mRNA capping enzyme bound to the phosphorylated carboxy-terminal domain of RNA polymerase II. Mol. Cell *11*, 1549–1561.

Fairall, L., Schwabe, J.W., Chapman, L., Finch, J.T., and Rhodes, D. (1993). The crystal structure of a two zinc-finger peptide reveals an extension to the rules for zinc-finger/DNA recognition. Nature *366*, 483–487.

Fan, L., Arvai, A.S., Cooper, P.K., Iwai, S., Hanaoka, F., and Tainer, J.A. (2006). Conserved XPB core structure and motifs for DNA unwinding: implications for pathway selection of transcription or excision repair. Mol. Cell *22*, 27–37.

Feklistov, A., and Darst, S.A. (2011). Structural basis for promoter-10 element recognition by the bacterial RNA polymerase σ subunit. Cell *147*, 1257–1269.

Fernández-Tornero, C., Moreno-Morcillo, M., Rashid, U.J., Taylor, N.M., Ruiz, F.M., Gruene, T., Legrand, P., Steuerwald, U., and Müller, C.W. (2013). Crystal structure of the 14-subunit RNA polymerase I. Nature *502*, 644–649.

Filippakopoulos, P., Qi, J., Picaud, S., Shen, Y., Smith, W.B., Fedorov, O., Morse, E.M., Keates, T., Hickman, T.T., Felletar, I., et al. (2010). Selective inhibition of BET bromodomains. Nature *468*, 1067–1073.

Finnin, M.S., Donigian, J.R., Cohen, A., Richon, V.M., Rifkind, R.A., Marks, P.A., Breslow, R., and Pavletich, N.P. (1999). Structures of a histone deacetylase homologue bound to the TSA and SAHA inhibitors. Nature *401*, 188–193.

Finnin, M.S., Donigian, J.R., and Pavletich, N.P. (2001). Structure of the histone deacetylase SIRT2. Nat. Struct. Biol. *8*, 621–625.

Friedman, A.M., Fischmann, T.O., and Steitz, T.A. (1995). Crystal structure of lac repressor core tetramer and its implications for DNA looping. Science *268*, 1721–1727.

Geiger, J.H., Hahn, S., Lee, S., and Sigler, P.B. (1996). Crystal structure of the yeast TFIIA/TBP/DNA complex. Science *272*, 830–836.

Ghosh, G., van Duyne, G., Ghosh, S., and Sigler, P.B. (1995). Structure of NF-kappa B p50 homodimer bound to a kappa B site. Nature *373*, 303–310.

Ghosh, A., Shuman, S., and Lima, C.D. (2008). The structure of Fcp1, an essential RNA polymerase II CTD phosphatase. Mol. Cell *32*, 478–490.

Gibbons, B.J., Brignole, E.J., Azubel, M., Murakami, K., Voss, N.R., Bushnell, D.A., Asturias, F.J., and Kornberg, R.D. (2012). Subunit architecture of general transcription factor TFIIH. Proc. Natl. Acad. Sci. USA *109*, 1949–1954.

Gingras, A.C., Gstaiger, M., Raught, B., and Aebersold, R. (2007). Analysis of protein complexes using mass spectrometry. Nat. Rev. Mol. Cell Biol. *8*, 645–654.

Gnatt, A.L., Cramer, P., Fu, J., Bushnell, D.A., and Kornberg, R.D. (2001). Structural basis of transcription: an RNA polymerase II elongation complex at 3.3 A resolution. Science *292*, 1876–1882.

Grünberg, S., Warfield, L., and Hahn, S. (2012). Architecture of the RNA polymerase II preinitiation complex and mechanism of ATP-dependent promoter opening. Nat. Struct. Mol. Biol. *19*, 788–796.

Hauk, G., McKnight, J.N., Nodelman, I.M., and Bowman, G.D. (2010). The chromodomains of the Chd1 chromatin remodeler regulate DNA access to the ATPase motor. Mol. Cell *39*, 711–723.

He, Y., Fang, J., Taatjes, D.J., and Nogales, E. (2013). Structural visualization of key steps in human transcription initiation. Nature *495*, 481–486.

Hirata, A., Klein, B.J., and Murakami, K.S. (2008). The X-ray crystal structure of RNA polymerase from Archaea. Nature *451*, 851–854.

Hondele, M., Stuwe, T., Hassler, M., Halbach, F., Bowman, A., Zhang, E.T., Nijmeijer, B., Kotthoff, C., Rybin, V., Amlacher, S., et al. (2013). Structural basis of histone H2A-H2B recognition by the essential chaperone FACT. Nature *499*, 111–114.

Hu, H., Liu, Y., Wang, M., Fang, J., Huang, H., Yang, N., Li, Y., Wang, J., Yao, X., Shi, Y., et al. (2011). Structure of a CENP-A-histone H4 heterodimer in complex with chaperone HJURP. Genes Dev. *25*, 901–906.

Huxford, T., Huang, D.B., Malek, S., and Ghosh, G. (1998). The crystal structure of the IkappaBalpha/NF-kappaB complex reveals mechanisms of NF-kappaB inactivation. Cell *95*, 759–770.

Imasaki, T., Calero, G., Cai, G., Tsai, K.L., Yamada, K., Cardelli, F., Erdjument-Bromage, H., Tempst, P., Berger, I., Kornberg, G.L., et al. (2011). Architecture of the Mediator head module. Nature *475*, 240–243.

Jacobs, S.A., and Khorasanizadeh, S. (2002). Structure of HP1 chromodomain bound to a lysine 9-methylated histone H3 tail. Science *295*, 2080–2083.

Jacobson, R.H., Ladurner, A.G., King, D.S., and Tjian, R. (2000). Structure and function of a human TAFII250 double bromodomain module. Science *288*, 1422–1425.

Jain, D., Nickels, B.E., Sun, L., Hochschild, A., and Darst, S.A. (2004). Structure of a ternary transcription activation complex. Mol. Cell *13*, 45–53.

Jeruzalmi, D., and Steitz, T.A. (1998). Structure of T7 RNA polymerase complexed to the transcriptional inhibitor T7 lysozyme. EMBO J. *17*, 4101–4113.

Jordan, S.R., and Pabo, C.O. (1988). Structure of the lambda complex at 2.5 A resolution: details of the repressor-operator interactions. Science *242*, 893–899.

Kamenski, T., Heilmeier, S., Meinhart, A., and Cramer, P. (2004). Structure and mechanism of RNA polymerase II CTD phosphatases. Mol. Cell *15*, 399–407.

Kettenberger, H., Armache, K.J., and Cramer, P. (2003). Architecture of the RNA polymerase II-TFIIS complex and implications for mRNA cleavage. Cell *114*, 347–357.

Kim, J.L., Nikolov, D.B., and Burley, S.K. (1993a). Co-crystal structure of TBP recognizing the minor groove of a TATA element. Nature *365*, 520–527.

Kim, Y., Geiger, J.H., Hahn, S., and Sigler, P.B. (1993b). Crystal structure of a yeast TBP/TATA-box complex. Nature *365*, 512–520.

Kissinger, C.R., Liu, B.S., Martin-Blanco, E., Kornberg, T.B., and Pabo, C.O. (1990). Crystal structure of an engrailed homeodomain-DNA complex at 2.8 A resolution: a framework for understanding homeodomain-DNA interactions. Cell *63*, 579–590.

Klimasauskas, S., Kumar, S., Roberts, R.J., and Cheng, X. (1994). HhaI methyltransferase flips its target base out of the DNA helix. Cell *76*, 357–369.

Köhler, A., Zimmerman, E., Schneider, M., Hurt, E., and Zheng, N. (2010). Structural basis for assembly and activation of the heterotetrameric SAGA histone H2B deubiquitinase module. Cell *141*, 606–617.

König, P., and Richmond, T.J. (1993). The X-ray structure of the GCN4-bZIP bound to ATF/CREB site DNA shows the complex depends on DNA flexibility. J. Mol. Biol. *233*, 139–154.

Korkhin, Y., Unligil, U.M., Littlefield, O., Nelson, P.J., Stuart, D.I., Sigler, P.B., Bell, S.D., and Abrescia, N.G. (2009). Evolution of complex RNA polymerases: the complete archaeal RNA polymerase structure. PLoS Biol. *7*, e1000102.

Kostrewa, D., Zeller, M.E., Armache, K.J., Seizl, M., Leike, K., Thomm, M., and Cramer, P. (2009). RNA polymerase II-TFIIB structure and mechanism of transcription initiation. Nature *462*, 323–330.

Kühlbrandt, W. (2014). Biochemistry. The resolution revolution. Science *343*, 1443–1444.

Kussie, P.H., Gorina, S., Marechal, V., Elenbaas, B., Moreau, J., Levine, A.J., and Pavletich, N.P. (1996). Structure of the MDM2 oncoprotein bound to the p53 tumor suppressor transactivation domain. Science *274*, 948–953.

Kwon, T., Chang, J.H., Kwak, E., Lee, C.W., Joachimiak, A., Kim, Y.C., Lee, J., and Cho, Y. (2003). Mechanism of histone lysine methyl transfer revealed by the structure of SET7/9-AdoMet. EMBO J. *22*, 292–303.

Larivière, L., Plaschka, C., Seizl, M., Wenzeck, L., Kurth, F., and Cramer, P. (2012). Structure of the Mediator head module. Nature *492*, 448–451.

Lesser, D.R., Kurpiewski, M.R., and Jen-Jacobson, L. (1990). The energetic basis of specificity in the Eco RI endonuclease—DNA interaction. Science *250*, 776–786.

Leurent, C., Sanders, S., Ruhlmann, C., Mallouh, V., Weil, P.A., Kirschner, D.B., Tora, L., and Schultz, P. (2002). Mapping histone fold TAFs within yeast TFIID. EMBO J. *21*, 3424–3433.

Lewis, M., Chang, G., Horton, N.C., Kercher, M.A., Pace, H.C., Schumacher, M.A., Brennan, R.G., and Lu, P. (1996). Crystal structure of the lactose operon repressor and its complexes with DNA and inducer. Science *271*, 1247–1254.

Li, T., Stark, M.R., Johnson, A.D., and Wolberger, C. (1995). Crystal structure of the MATa1/MAT alpha 2 homeodomain heterodimer bound to DNA. Science *270*, 262–269.

Li, H., Ilin, S., Wang, W., Duncan, E.M., Wysocka, J., Allis, C.D., and Patel, D.J. (2006). Molecular basis for site-specific read-out of histone H3K4me3 by the BPTF PHD finger of NURF. Nature *442*, 91–95.

Liu, X., Wang, L., Zhao, K., Thompson, P.R., Hwang, Y., Marmorstein, R., and Cole, P.A. (2008). The structural basis of protein acetylation by the p300/CBP transcriptional coactivator. Nature *451*, 846–850.

Liu, X., Bushnell, D.A., Wang, D., Calero, G., and Kornberg, R.D. (2010). Structure of an RNA polymerase II-TFIIB complex and the transcription initiation mechanism. Science *327*, 206–209.

Lolli, G., Lowe, E.D., Brown, N.R., and Johnson, L.N. (2004). The crystal structure of human CDK7 and its protein recognition properties. Structure *12*, 2067–2079.

Luger, K., Mäder, A.W., Richmond, R.K., Sargent, D.F., and Richmond, T.J. (1997). Crystal structure of the nucleosome core particle at 2.8 A resolution. Nature *389*, 251–260.

Luisi, B.F., Xu, W.X., Otwinowski, Z., Freedman, L.P., Yamamoto, K.R., and Sigler, P.B. (1991). Crystallographic analysis of the interaction of the glucocorticoid receptor with DNA. Nature *352*, 497–505.

Makde, R.D., England, J.R., Yennawar, H.P., and Tan, S. (2010). Structure of RCC1 chromatin factor bound to the nucleosome core particle. Nature *467*, 562–566.

Malhotra, A., Severinova, E., and Darst, S.A. (1996). Crystal structure of a sigma 70 subunit fragment from E. coli RNA polymerase. Cell *87*, 127–136.

Marmorstein, R., Carey, M., Ptashne, M., and Harrison, S.C. (1992). DNA recognition by GAL4: structure of a protein-DNA complex. Nature *356*, 408–414.

McKay, D.B., and Steitz, T.A. (1981). Structure of catabolite gene activator protein at 2.9 A resolution suggests binding to left-handed B-DNA. Nature *290*, 744–749.

Meinhart, A., and Cramer, P. (2004). Recognition of RNA polymerase II carboxy-terminal domain by 3′-RNA-processing factors. Nature *430*, 223–226.

Meyer, K.D., Lin, S.C., Bernecky, C., Gao, Y., and Taatjes, D.J. (2010). p53 activates transcription by directing structural shifts in Mediator. Nat. Struct. Mol. Biol. *17*, 753–760.

Min, J., Landry, J., Sternglanz, R., and Xu, R.M. (2001). Crystal structure of a SIR2 homolog-NAD complex. Cell *105*, 269–279.

Min, J., Zhang, X., Cheng, X., Grewal, S.I., and Xu, R.M. (2002). Structure of the SET domain histone lysine methyltransferase Clr4. Nat. Struct. Biol. *9*, 828–832.

Morinière, J., Rousseaux, S., Steuerwald, U., Soler-López, M., Curtet, S., Vitte, A.L., Govin, J., Gaucher, J., Sadoul, K., Hart, D.J., et al. (2009). Cooperative binding of two acetylation marks on a histone tail by a single bromodomain. Nature *461*, 664–668.

Mühlbacher, W., Sainsbury, S., Hemann, M., Hantsche, M., Neyer, S., Herzog, F., and Cramer, P. (2014). Conserved architecture of the core RNA polymerase II initiation complex. Nat. Commun. *5*, 4310.

Müller, C.W., Rey, F.A., Sodeoka, M., Verdine, G.L., and Harrison, S.C. (1995). Structure of the NF-kappa B p50 homodimer bound to DNA. Nature *373*, 311–317.

Murakami, K.S., Masuda, S., Campbell, E.A., Muzzin, O., and Darst, S.A. (2002a). Structural basis of transcription initiation: an RNA polymerase holoenzyme-DNA complex. Science *296*, 1285–1290.

Murakami, K.S., Masuda, S., and Darst, S.A. (2002b). Structural basis of transcription initiation: RNA polymerase holoenzyme at 4 A resolution. Science *296*, 1280–1284.

Murakami, K., Elmlund, H., Kalisman, N., Bushnell, D.A., Adams, C.M., Azubel, M., Elmlund, D., Levi-Kalisman, Y., Liu, X., Gibbons, B.J., et al. (2013). Architecture of an RNA polymerase II transcription pre-initiation complex. Science *342*, 1238724.

Naumova, N., Imakaev, M., Fudenberg, G., Zhan, Y., Lajoie, B.R., Mirny, L.A., and Dekker, J. (2013). Organization of the mitotic chromosome. Science *342*, 948–953.

Ng, S.S., Kavanagh, K.L., McDonough, M.A., Butler, D., Pilka, E.S., Lienard, B.M., Bray, J.E., Savitsky, P., Gileadi, O., von Delft, F., et al. (2007). Crystal structures of histone demethylase JMJD2A reveal basis for substrate specificity. Nature *448*, 87–91.

Ngo, H.B., Kaiser, J.T., and Chan, D.C. (2011). The mitochondrial transcription and packaging factor Tfam imposes a U-turn on mitochondrial DNA. Nat. Struct. Mol. Biol. *18*, 1290–1296.

Nguyen, V.Q., Ranjan, A., Stengel, F., Wei, D., Aebersold, R., Wu, C., and Leschziner, A.E. (2013). Molecular architecture of the ATP-dependent chromatin-remodeling complex SWR1. Cell *154*, 1220–1231.

Nikolov, D.B., Hu, S.H., Lin, J., Gasch, A., Hoffmann, A., Horikoshi, M., Chua, N.H., Roeder, R.G., and Burley, S.K. (1992). Crystal structure of TFIID TATA-box binding protein. Nature *360*, 40–46.

Nikolov, D.B., Chen, H., Halay, E.D., Usheva, A.A., Hisatake, K., Lee, D.K., Roeder, R.G., and Burley, S.K. (1995). Crystal structure of a TFIIB-TBP-TATA-element ternary complex. Nature *377*, 119–128.

Obri, A., Ouararhni, K., Papin, C., Diebold, M.L., Padmanabhan, K., Marek, M., Stoll, I., Roy, L., Reilly, P.T., Mak, T.W., et al. (2014). ANP32E is a histone chaperone that removes H2A.Z from chromatin. Nature *505*, 648–653.

Opalka, N., Chlenov, M., Chacon, P., Rice, W.J., Wriggers, W., and Darst, S.A. (2003). Structure and function of the transcription elongation factor GreB bound to bacterial RNA polymerase. Cell *114*, 335–345.

Otting, G., Qian, Y.Q., Billeter, M., Müller, M., Affolter, M., Gehring, W.J., and Wüthrich, K. (1990). Protein—DNA contacts in the structure of a homeodomain—DNA complex determined by nuclear magnetic resonance spectroscopy in solution. EMBO J. *9*, 3085–3092.

Otwinowski, Z., Schevitz, R.W., Zhang, R.G., Lawson, C.L., Joachimiak, A., Marmorstein, R.Q., Luisi, B.F., and Sigler, P.B. (1988). Crystal structure of trp repressor/operator complex at atomic resolution. Nature *335*, 321–329.

Owen, D.J., Ornaghi, P., Yang, J.C., Lowe, N., Evans, P.R., Ballario, P., Neuhaus, D., Filetici, P., and Travers, A.A. (2000). The structural basis for the recognition of acetylated histone H4 by the bromodomain of histone acetyltransferase gcn5p. EMBO J. *19*, 6141–6149.

Pabo, C.O., and Lewis, M. (1982). The operator-binding domain of lambda repressor: structure and DNA recognition. Nature *298*, 443–447.

Panne, D., Maniatis, T., and Harrison, S.C. (2007). An atomic model of the interferon-beta enhanceosome. Cell *129*, 1111–1123.

Park, Y.J., and Luger, K. (2006). The structure of nucleosome assembly protein 1. Proc. Natl. Acad. Sci. USA *103*, 1248–1253.

Pavletich, N.P., and Pabo, C.O. (1991). Zinc finger-DNA recognition: crystal structure of a Zif268-DNA complex at 2.1 A. Science *252*, 809–817.

Peña, P.V., Davrazou, F., Shi, X., Walter, K.L., Verkhusha, V.V., Gozani, O., Zhao, R., and Kutateladze, T.G. (2006). Molecular mechanism of histone H3K4me3 recognition by plant homeodomain of ING2. Nature *442*, 100–103.

Piper, D.E., Batchelor, A.H., Chang, C.P., Cleary, M.L., and Wolberger, C. (1999). Structure of a HoxB1-Pbx1 heterodimer bound to DNA: role of the hexapeptide and a fourth homeodomain helix in complex formation. Cell *96*, 587–597.

Qian, Y.Q., Billeter, M., Otting, G., Müller, M., Gehring, W.J., and Wüthrich, K. (1989). The structure of the Antennapedia homeodomain determined by NMR spectroscopy in solution: comparison with prokaryotic repressors. Cell *59*, 573–580.

Racki, L.R., Naber, N., Pate, E., Leonard, J.D., Cooke, R., and Narlikar, G.J. (2014). The histone H4 tail regulates the conformation of the ATP-binding pocket in the SNF2h chromatin remodeling enzyme. J. Mol. Biol. *426*, 2034–2044.

Radhakrishnan, I., Pérez-Alvarado, G.C., Parker, D., Dyson, H.J., Montminy, M.R., and Wright, P.E. (1997). Solution structure of the KIX domain of CBP bound to the transactivation domain of CREB: a model for activator:coactivator interactions. Cell *91*, 741–752.

Reményi, A., Lins, K., Nissen, L.J., Reinbold, R., Schöler, H.R., and Wilmanns, M. (2003). Crystal structure of a POU/HMG/DNA ternary complex suggests differential assembly of Oct4 and Sox2 on two enhancers. Genes Dev. *17*, 2048–2059.

Rice, P.A., Yang, S., Mizuuchi, K., and Nash, H.A. (1996). Crystal structure of an IHF-DNA complex: a protein-induced DNA U-turn. Cell *87*, 1295–1306.

Richmond, T.J., Finch, J.T., Rushton, B., Rhodes, D., and Klug, A. (1984). Structure of the nucleosome core particle at 7 A resolution. Nature *311*, 532–537.

Ringel, R., Sologub, M., Morozov, Y.I., Litonin, D., Cramer, P., and Temiakov, D. (2011). Structure of human mitochondrial RNA polymerase. Nature *478*, 269–273.

Robertus, J.D., Ladner, J.E., Finch, J.T., Rhodes, D., Brown, R.S., Clark, B.F., and Klug, A. (1974). Structure of yeast phenylalanine tRNA at 3 A resolution. Nature *250*, 546–551.

Robinson, P.J., Fairall, L., Huynh, V.A., and Rhodes, D. (2006). EM measurements define the dimensions of the "30-nm" chromatin fiber: evidence for a compact, interdigitated structure. Proc. Natl. Acad. Sci. USA *103*, 6506–6511.

Robinson, P.J., Bushnell, D.A., Trnka, M.J., Burlingame, A.L., and Kornberg, R.D. (2012). Structure of the mediator head module bound to the carboxy-terminal domain of RNA polymerase II. Proc. Natl. Acad. Sci. USA *109*, 17931–17935.

Rojas, J.R., Trievel, R.C., Zhou, J., Mo, Y., Li, X., Berger, S.L., Allis, C.D., and Marmorstein, R. (1999). Structure of Tetrahymena GCN5 bound to coenzyme A and a histone H3 peptide. Nature *401*, 93–98.

Rubio-Cosials, A., Sidow, J.F., Jiménez-Menéndez, N., Fernández-Millán, P., Montoya, J., Jacobs, H.T., Coll, M., Bernadó, P., and Solà, M. (2011). Human mitochondrial transcription factor A induces a U-turn structure in the light strand promoter. Nat. Struct. Mol. Biol. *18*, 1281–1289.

Sainsbury, S., Niesser, J., and Cramer, P. (2013). Structure and function of the initially transcribing RNA polymerase II-TFIIB complex. Nature *493*, 437–440.

Samara, N.L., Datta, A.B., Berndsen, C.E., Zhang, X., Yao, T., Cohen, R.E., and Wolberger, C. (2010). Structural insights into the assembly and function of the SAGA deubiquitinating module. Science *328*, 1025–1029.

Saravanan, M., Wuerges, J., Bose, D., McCormack, E.A., Cook, N.J., Zhang, X., and Wigley, D.B. (2012). Interactions between the nucleosome histone core and Arp8 in the INO80 chromatin remodeling complex. Proc. Natl. Acad. Sci. USA *109*, 20883–20888.

Schalch, T., Duda, S., Sargent, D.F., and Richmond, T.J. (2005). X-ray structure of a tetranucleosome and its implications for the chromatin fibre. Nature *436*, 138–141.

Scheffer, M.P., Eltsov, M., and Frangakis, A.S. (2011). Evidence for short-range helical order in the 30-nm chromatin fibers of erythrocyte nuclei. Proc. Natl. Acad. Sci. USA *108*, 16992–16997.

Schevitz, R.W., Otwinowski, Z., Joachimiak, A., Lawson, C.L., and Sigler, P.B. (1985). The three-dimensional structure of trp repressor. Nature *317*, 782–786.

Schneider, E.V., Böttcher, J., Blaesse, M., Neumann, L., Huber, R., and Maskos, K. (2011). The structure of CDK8/CycC implicates specificity in the CDK/cyclin family and reveals interaction with a deep pocket binder. J. Mol. Biol. *412*, 251–266.

Schuetz, A., Nana, D., Rose, C., Zocher, G., Milanovic, M., Koenigsmann, J., Blasig, R., Heinemann, U., and Carstanjen, D. (2011). The structure of the Klf4 DNA-binding domain links to self-renewal and macrophage differentiation. Cell. Mol. Life Sci. *68*, 3121–3131.

Schultz, S.C., Shields, G.C., and Steitz, T.A. (1991). Crystal structure of a CAP-DNA complex: the DNA is bent by 90 degrees. Science *253*, 1001–1007.

Schultz, P., Fribourg, S., Poterszman, A., Mallouh, V., Moras, D., and Egly, J.M. (2000). Molecular structure of human TFIIH. Cell *102*, 599–607.

Schwabe, J.W., Chapman, L., Finch, J.T., and Rhodes, D. (1993). The crystal structure of the estrogen receptor DNA-binding domain bound to DNA: how receptors discriminate between their response elements. Cell *75*, 567–578.

Schwinghammer, K., Cheung, A.C., Morozov, Y.I., Agaronyan, K., Temiakov, D., and Cramer, P. (2013). Structure of human mitochondrial RNA polymerase elongation complex. Nat. Struct. Mol. Biol. *20*, 1298–1303.

Serpa, J.J., Parker, C.E., Petrotchenko, E.V., Han, J., Pan, J., and Borchers, C.H. (2012). Mass spectrometry-based structural proteomics. Eur. J. Mass Spectrom. (Chichester, Eng.) *18*, 251–267.

Shakked, Z., Rabinovich, D., Cruse, W.B., Egert, E., Kennard, O., Sala, G., Salisbury, S.A., and Viswamitra, M.A. (1981). Crystalline A-dna: the X-ray analysis of the fragment d(G-G-T-A-T-A-C-C). Proc. R. Soc. Lond. B Biol. Sci. *213*, 479–487.

Shi, Y. (2014). A glimpse of structural biology through X-ray crystallography. Cell *159*, this issue, 995–1014.

Shiau, A.K., Barstad, D., Loria, P.M., Cheng, L., Kushner, P.J., Agard, D.A., and Greene, G.L. (1998). The structural basis of estrogen receptor/coactivator recognition and the antagonism of this interaction by tamoxifen. Cell *95*, 927–937.

Somoza, J.R., Skene, R.J., Katz, B.A., Mol, C., Ho, J.D., Jennings, A.J., Luong, C., Arvai, A., Buggy, J.J., Chi, E., et al. (2004). Structural snapshots of human HDAC8 provide insights into the class I histone deacetylases. Structure *12*, 1325–1334.

Song, J., Rechkoblit, O., Bestor, T.H., and Patel, D.J. (2011). Structure of DNMT1-DNA complex reveals a role for autoinhibition in maintenance DNA methylation. Science *331*, 1036–1040.

Song, J., Teplova, M., Ishibe-Murakami, S., and Patel, D.J. (2012). Structure-based mechanistic insights into DNMT1-mediated maintenance DNA methylation. Science *335*, 709–712.

Song, F., Chen, P., Sun, D., Wang, M., Dong, L., Liang, D., Xu, R.M., Zhu, P., and Li, G. (2014). Cryo-EM study of the chromatin fiber reveals a double helix twisted by tetranucleosomal units. Science *344*, 376–380.

Sousa, R., Chung, Y.J., Rose, J.P., and Wang, B.C. (1993). Crystal structure of bacteriophage T7 RNA polymerase at 3.3 A resolution. Nature *364*, 593–599.

Stavropoulos, P., Blobel, G., and Hoelz, A. (2006). Crystal structure and mechanism of human lysine-specific demethylase-1. Nat. Struct. Mol. Biol. *13*, 626–632.

Steitz, T.A., and Steitz, J.A. (1993). A general two-metal-ion mechanism for catalytic RNA. Proc. Natl. Acad. Sci. USA *90*, 6498–6502.

Strahl, B.D., and Allis, C.D. (2000). The language of covalent histone modifications. Nature *403*, 41–45.

Suto, R.K., Clarkson, M.J., Tremethick, D.J., and Luger, K. (2000). Crystal structure of a nucleosome core particle containing the variant histone H2A.Z. Nat. Struct. Biol. *7*, 1121–1124.

Szymborska, A., de Marco, A., Daigle, N., Cordes, V.C., Briggs, J.A., and Ellenberg, J. (2013). Nuclear pore scaffold structure analyzed by super-resolution microscopy and particle averaging. Science *341*, 655–658.

Taatjes, D.J., Näär, A.M., Andel, F., 3rd, Nogales, E., and Tjian, R. (2002). Structure, function, and activator-induced conformations of the CRSP coactivator. Science *295*, 1058–1062.

Tachiwana, H., Kagawa, W., Shiga, T., Osakabe, A., Miya, Y., Saito, K., Hayashi-Takanaka, Y., Oda, T., Sato, M., Park, S.Y., et al. (2011). Crystal structure of the human centromeric nucleosome containing CENP-A. Nature *476*, 232–235.

Tahirov, T.H., Temiakov, D., Anikin, M., Patlan, V., McAllister, W.T., Vassylyev, D.G., and Yokoyama, S. (2002). Structure of a T7 RNA polymerase elongation complex at 2.9 A resolution. Nature *420*, 43–50.

Tahirov, T.H., Babayeva, N.D., Varzavand, K., Cooper, J.J., Sedore, S.C., and Price, D.H. (2010). Crystal structure of HIV-1 Tat complexed with human P-TEFb. Nature *465*, 747–751.

Tan, S., and Richmond, T.J. (1998). Crystal structure of the yeast MATalpha2/MCM1/DNA ternary complex. Nature *391*, 660–666.

Tan, S., Hunziker, Y., Sargent, D.F., and Richmond, T.J. (1996). Crystal structure of a yeast TFIIA/TBP/DNA complex. Nature *381*, 127–151.

Temiakov, D., Patlan, V., Anikin, M., McAllister, W.T., Yokoyama, S., and Vassylyev, D.G. (2004). Structural basis for substrate selection by t7 RNA polymerase. Cell *116*, 381–391.

Thomä, N.H., Czyzewski, B.K., Alexeev, A.A., Mazin, A.V., Kowalczykowski, S.C., and Pavletich, N.P. (2005). Structure of the SWI2/SNF2 chromatin-remodeling domain of eukaryotic Rad54. Nat. Struct. Mol. Biol. *12*, 350–356.

Tosi, A., Haas, C., Herzog, F., Gilmozzi, A., Berninghausen, O., Ungewickell, C., Gerhold, C.B., Lakomek, K., Aebersold, R., Beckmann, R., and Hopfner, K.P. (2013). Structure and subunit topology of the INO80 chromatin remodeler and its nucleosome complex. Cell *154*, 1207–1219.

Tsai, W.W., Wang, Z., Yiu, T.T., Akdemir, K.C., Xia, W., Winter, S., Tsai, C.Y., Shi, X., Schwarzer, D., Plunkett, W., et al. (2010). TRIM24 links a non-canonical histone signature to breast cancer. Nature *468*, 927–932.

Tsai, K.L., Tomomori-Sato, C., Sato, S., Conaway, R.C., Conaway, J.W., and Asturias, F.J. (2014). Subunit architecture and functional modular rearrangements of the transcriptional mediator complex. Cell *157*, 1430–1444.

Vannini, A., Volpari, C., Filocamo, G., Casavola, E.C., Brunetti, M., Renzoni, D., Chakravarty, P., Paolini, C., De Francesco, R., Gallinari, P., et al. (2004). Crystal structure of a eukaryotic zinc-dependent histone deacetylase, human HDAC8, complexed with a hydroxamic acid inhibitor. Proc. Natl. Acad. Sci. USA *101*, 15064–15069.

Vassylyev, D.G., Sekine, S., Laptenko, O., Lee, J., Vassylyeva, M.N., Borukhov, S., and Yokoyama, S. (2002). Crystal structure of a bacterial RNA polymerase holoenzyme at 2.6 A resolution. Nature *417*, 712–719.

Vassylyev, D.G., Vassylyeva, M.N., Zhang, J., Palangat, M., Artsimovitch, I., and Landick, R. (2007). Structural basis for substrate loading in bacterial RNA polymerase. Nature *448*, 163–168.

Verdecia, M.A., Bowman, M.E., Lu, K.P., Hunter, T., and Noel, J.P. (2000). Structural basis for phosphoserine-proline recognition by group IV WW domains. Nat. Struct. Biol. *7*, 639–643.

Vermeulen, M., Mulder, K.W., Denissov, S., Pijnappel, W.W., van Schaik, F.M., Varier, R.A., Baltissen, M.P., Stunnenberg, H.G., Mann, M., and Timmers, H.T. (2007). Selective anchoring of TFIID to nucleosomes by trimethylation of histone H3 lysine 4. Cell *131*, 58–69.

Wang, A.H., Quigley, G.J., Kolpak, F.J., Crawford, J.L., van Boom, J.H., van der Marel, G., and Rich, A. (1979). Molecular structure of a left-handed double helical DNA fragment at atomic resolution. Nature *282*, 680–686.

Wang, D., Bushnell, D.A., Westover, K.D., Kaplan, C.D., and Kornberg, R.D. (2006). Structural basis of transcription: role of the trigger loop in substrate specificity and catalysis. Cell *127*, 941–954.

Wang, X., Sun, Q., Ding, Z., Ji, J., Wang, J., Kong, X., Yang, J., and Cai, G. (2014). Redefining the modular organization of the core Mediator complex. Cell Res. *24*, 796–808.

Watson, J.D., and Crick, F.H. (1953). Molecular structure of nucleic acids; a structure for deoxyribose nucleic acid. Nature *171*, 737–738.

Wilson, J.R., Jing, C., Walker, P.A., Martin, S.R., Howell, S.A., Blackburn, G.M., Gamblin, S.J., and Xiao, B. (2002). Crystal structure and functional analysis of the histone methyltransferase SET7/9. Cell *111*, 105–115.

Wing, R., Drew, H., Takano, T., Broka, C., Tanaka, S., Itakura, K., and Dickerson, R.E. (1980). Crystal structure analysis of a complete turn of B-DNA. Nature *287*, 755–758.

Wolberger, C., Dong, Y.C., Ptashne, M., and Harrison, S.C. (1988). Structure of a phage 434 Cro/DNA complex. Nature *335*, 789–795.

Wong, W., Bai, X.C., Brown, A., Fernandez, I.S., Hanssen, E., Condron, M., Tan, Y.H., Baum, J., and Scheres, S.H. (2014). Cryo-EM structure of the Plasmodium falciparum 80S ribosome bound to the anti-protozoan drug emetine. eLife *3*, e03080.

Xi, Q., Wang, Z., Zaromytidou, A.I., Zhang, X.H., Chow-Tsang, L.F., Liu, J.X., Kim, H., Barlas, A., Manova-Todorova, K., Kaartinen, V., et al. (2011). A poised chromatin platform for TGF-β access to master regulators. Cell *147*, 1511–1524.

Xiang, K., Nagaike, T., Xiang, S., Kilic, T., Beh, M.M., Manley, J.L., and Tong, L. (2010). Crystal structure of the human symplekin-Ssu72-CTD phosphopeptide complex. Nature *467*, 729–733.

Xiao, B., Jing, C., Wilson, J.R., Walker, P.A., Vasisht, N., Kelly, G., Howell, S., Taylor, I.A., Blackburn, G.M., and Gamblin, S.J. (2003). Structure and catalytic mechanism of the human histone methyltransferase SET7/9. Nature *421*, 652–656.

Xu, K., Zhong, G., and Zhuang, X. (2013). Actin, spectrin, and associated proteins form a periodic cytoskeletal structure in axons. Science *339*, 452–456.

Yamada, K., Frouws, T.D., Angst, B., Fitzgerald, D.J., DeLuca, C., Schimmele, K., Sargent, D.F., and Richmond, T.J. (2011). Structure and mechanism of the chromatin remodelling factor ISW1a. Nature *472*, 448–453.

Yang, M., Gocke, C.B., Luo, X., Borek, D., Tomchick, D.R., Machius, M., Otwinowski, Z., and Yu, H. (2006). Structural basis for CoREST-dependent demethylation of nucleosomes by the human LSD1 histone demethylase. Mol. Cell *23*, 377–387.

Yin, Y.W., and Steitz, T.A. (2002). Structural basis for the transition from initiation to elongation transcription in T7 RNA polymerase. Science *298*, 1387–1395.

Zhang, G., Campbell, E.A., Minakhin, L., Richter, C., Severinov, K., and Darst, S.A. (1999). Crystal structure of Thermus aquaticus core RNA polymerase at 3.3 A resolution. Cell *98*, 811–824.

Zhang, X., Tamaru, H., Khan, S.I., Horton, J.R., Keefe, L.J., Selker, E.U., and Cheng, X. (2002). Structure of the Neurospora SET domain protein DIM-5, a histone H3 lysine methyltransferase. Cell *111*, 117–127.

Zhang, Y., Feng, Y., Chatterjee, S., Tuske, S., Ho, M.X., Arnold, E., and Ebright, R.H. (2012). Structural basis of transcription initiation. Science *338*, 1076–1080.